Phenotyping cardiometabolic disease with magnetic resonance techniques

Paiman, E.H.M.

CHAPTER

2

The role of insulin resistance in the relation of visceral, abdominal subcutaneous and total body fat to cardiovascular function

Paiman EHM, de Mutsert R, Widya RL, Rosendaal FR, Jukema JW, Lamb HJ

Nutr Metab Cardiovasc Dis. 2020; in press. doi: 10.1016/j.numecd.2020.07.011

ABSTRACT

Background

The separate cardiovascular effects of type 2 diabetes and adiposity remain to be examined. This study aimed to investigate the role of insulin resistance in the relations of visceral (VAT), abdominal subcutaneous (aSAT) adipose tissue and total body fat (TBF) to cardiovascular remodeling.

Methods

In this cross-sectional analysis of the population-based Netherlands Epidemiology of Obesity study, 914 middle-aged individuals (46% men) were included. Participants underwent magnetic resonance imaging. Standardized linear regression coefficients (95%CI) were calculated, adjusted for potential confounding factors.

Results

All fat depots and insulin resistance (HOMA-IR), separate from VAT and TBF, were associated with lower mitral early and late peak filling rate ratios (E/A): -0.04 (-0.09;0.01) per SD (54 cm^2) VAT; -0.05 (-0.10;0.00) per SD (94 cm^2) aSAT; -0.09 (-0.16;-0.02) per SD (8%) TBF; -0.11 (-0.17;-0.05) per 10-fold increase in HOMA-IR, whereas VAT and TBF were differently associated with left ventricular (LV) end-diastolic volume: -8.9 (-11.7;-6.1) mL per SD VAT; +5.4 (1.1;9.7) mL per SD TBF. After adding HOMA-IR to the model to evaluate the mediating role of insulin resistance, change in E/A was -0.02 (-0.07;0.04) per SD VAT; -0.03 (-0.08;0.02) per SD aSAT; -0.06 (-0.13;0.01) per SD TBF, and change in LV end-diastolic volume was -7.0 (-9.7;-4.3) mL per SD VAT. In women, adiposity but not HOMA-IR was related to higher aortic arch pulse wave velocity.

Conclusion

Insulin resistance was associated with reduced diastolic function, separately from VAT and TBF, and partly mediated the associations between adiposity depots and lower diastolic function.

Highlights

- We examined the separate relations of HOMA-IR and body fat to cardiac remodeling.
- All adipose tissue depots were associated with reduced diastolic function.
- Visceral but not total body fat was related to a smaller left ventricular volume.
- HOMA-IR was linked to diastolic dysfunction, separately from body fat.
- HOMA-IR mediated the relation of body fat to diastolic dysfunction.

INTRODUCTION

Type 2 diabetes, in the absence of significant coronary artery disease, hypertension or other potential etiologies, is associated with myocardial remodeling (1). This concept is referred to as diabetic cardiomyopathy (2). Although diabetic cardiomyopathy has been recognized as a distinct clinical entity (3), its phenotypic characterization remains unclear (1). One of the difficulties in phenotyping diabetic cardiomyopathy is the strong association between obesity and type 2 diabetes (4). Due to their coexistence, it is challenging to isolate the contribution of type 2 diabetes and obesity to cardiovascular remodeling.

Obesity has been related to a variety of alterations in left ventricular (LV) morphology and function, vascular function and hemodynamics (5-9). Interestingly, visceral (VAT) and subcutaneous (SAT) adipose tissue are metabolically distinct and show differential incidence rates of cardiovascular disease (10). VAT in particular secretes proinflammatory and proatherogenic cytokines including tumor necrosis factor-alpha and interleukin-6 (11), whereas VAT produces less adiponectin, which protects the heart from adverse remodeling (12). Particularly VAT may predispose to type 2 diabetes, as low adiponectin levels and chronic inflammation are considered to mediate the effects of obesity in the pathogenesis of insulin resistance (13). Of importance, VAT and SAT appear to be differently associated with cardiac structure and hemodynamics (9,14). Overall obesity and SAT have been related to increases in LV dimensions and cardiac output, presumably as a result of intravascular volume expansion (9,14,15). In contrast, VAT has been associated with reduced LV end-diastolic volume and increased LV mass, possibly due to the release of prohypertrophic adipokines (9,14,16). Furthermore, previous large-scale studies have reported associations of type 2 diabetes with LV functional impairments, particularly diastolic dysfunction, but also with increased cardiac mass (17-21). Although VAT has been related to impaired diastolic function as well (22), a direct causal link between type 2 diabetes and diastolic dysfunction is supported by alterations in cardiac metabolism associated with insulin resistance (23-27). In contrast, LV morphological changes in type 2 diabetes may be explained predominantly by hemodynamic mechanisms associated with increased body size and altered body composition (9,28). Previously, only a few population-based studies have assessed imaging-based metrics of VAT and SAT in addition to generalized measures of obesity, when examining LV structure and function in obese individuals (9,14,29), but the association of type 2 diabetes with cardiovascular remodeling, separate from adipose tissue, remains to be investigated.

Furthermore, it has been demonstrated that not merely type 2 diabetes but rather the insulin resistance continuum has adverse effects on cardiac structure and function (17,18,30-33). As such, assessment of the role of insulin resistance in adipose tissue-related cardiovascular remodeling in the general population may contribute to the phenotypic characterization of diabetic cardiomyopathy. Thus far, the relation of insulin resistance to cardiovascular remodeling, independent of the body fat depots, has not been examined in a population-

based cohort, whereas adjustment for overall obesity may not fully separate the cardiovascular effects of insulin resistance and VAT.

The aim of this study was to investigate the role of insulin resistance in the associations of VAT, abdominal SAT (aSAT) and total body fat (TBF) with cardiovascular remodeling, assessed by LV mass and dimensions, systolic and diastolic function, stroke volume, cardiac output and aortic stiffness, using magnetic resonance imaging (MRI), in the middle-aged general population. As depicted in **Figure 1**, this implies 1) assessment of the relation of insulin resistance to cardiovascular parameters after adjusting for potential confounding by adiposity, and 2) examination of the attenuation of the association of adiposity with cardiovascular parameters after adding insulin resistance as a potential mediator to the regression models. Our hypothesis is that insulin resistance is associated with reduced diastolic function, separately from VAT and TBF, and that insulin resistance is a mediator in the relation of adiposity to reduced diastolic function.

METHODS

Study design and study population

The Netherlands Epidemiology of Obesity (NEO) study is a prospective, population-based cohort study in 6,671 individuals (34). Between 2008 and 2012, men and women aged between 45 and 65 years, with a self-reported body mass index (BMI) of 27 kg/m^2 or higher, from Leiden and the surrounding area were invited to participate. To obtain a reference distribution of BMI, men and women from Leiderdorp in the same age range were invited irrespective of their BMI. A random subset of the participants underwent MRI. The Medical Ethics Committee of Leiden University Medical Center approved the study protocol. All participants provided written informed consent.

The present study is a cross-sectional analysis of the baseline measurements of the NEO study. Participants included those who underwent cardiac and abdominal MRI. Exclusion criteria were use of glucose-lowering medication (oral hypoglycemic agents or insulin) in the month before study visit and a history of cardiovascular disease (congestive heart failure, myocardial infarction, angina pectoris and/or heart rhythm abnormalities). Participants with missing data were excluded.

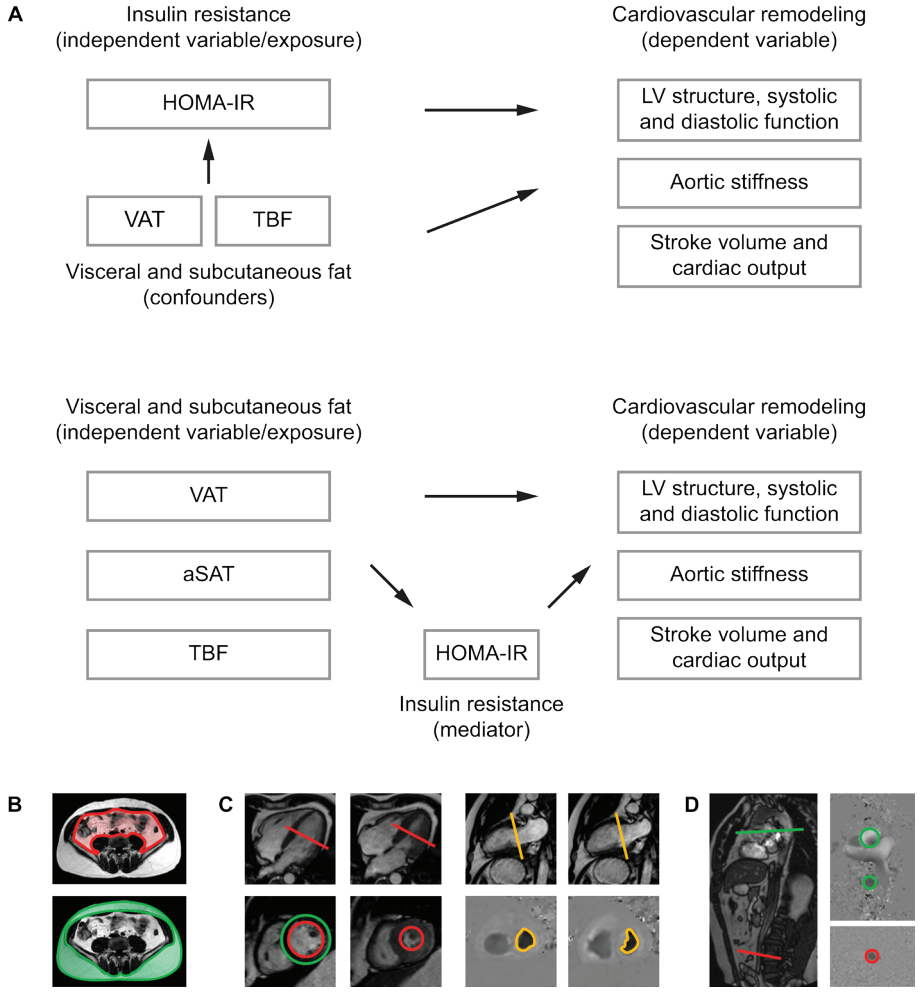

Figure 1. Study aim and MRI-derived adiposity and cardiovascular parameters. (**A**) This study sought to examine the role of HOMA-IR in the associations of VAT, aSAT and TBF with cardiovascular remodeling, assessed by LV mass and dimensions, systolic and diastolic function, stroke volume, cardiac output and aortic stiffness. (**B**) VAT (***upper image***) and aSAT (***lower image***) were assessed on transverse slices at the level of the fifth lumbar vertebra. (**C**) LV systolic function was quantified as the LV ejection fraction, derived from short-axis cine MRI. LV structure was assessed by measurement of LV mass and end-diastolic volumes (***left panel***). LV diastolic function was examined by calculating the ratio of the early and late diastolic flow rates across the mitral valve, using velocity-encoded MRI (***right panel***). (**D**) Aortic stiffness was quantified as the velocity of the systolic pulse wave, from ascending aorta to distal abdominal aorta, using velocity-encoded MRI. Abbreviations: aSAT: abdominal subcutaneous adipose tissue, HOMA-IR: homeostatic model assessment of insulin resistance, LV: left ventricular, TBF: total body fat, VAT: visceral adipose tissue.

Data collection

Self-reported ethnicity was categorized into white and other, education into low and high (higher vocational school, university and postgraduate education) and tobacco smoking into never (reference), former and current smoker. Physical activity was expressed in metabolic equivalents of task (MET)-hours per week. Data on the frequency, duration and intensity of physical activity during leisure time was collected using the Short Questionnaire to Assess Health-enhancing physical activity (SQUASH). In women, the use of hormones (contraceptives or hormone replacement therapy) was grouped into current and no use of estrogens and menopausal state into postmenopausal (reference), peri- and premenopausal. Data on anthropometry and blood pressure and blood samples were obtained in the morning after an overnight fast of at least ten hours. Hypertension was defined as systolic blood pressure ≥ 140 mmHg and/or diastolic blood pressure ≥ 90 mmHg, and/or use of antihypertensive drugs (35). Fasting glucose and insulin were examined using an enzymatic colorimetric assay (Roche Modular P800 Analyzer, Roche Diagnostics, Mannheim, Germany) and a two-site chemiluminescent immunometric assay (Siemens Immulite 2500, Siemens Healthcare Diagnostics, Breda), respectively. Details on the data collection can be found elsewhere (34).

Insulin resistance, adiposity and cardiovascular parameters

We used the homeostatic model assessment of insulin resistance (HOMA-IR). HOMA-IR was calculated according to: fasting glucose (in mmol/L) multiplied by fasting insulin (in mU/L), divided by 22.5 (36,37).

The MRI studies were at the same morning as the clinical data collection. Abdominal and cardiac MRI was performed on a 1.5 Tesla MR scanner (Philips Medical Systems, Best, the Netherlands). The MRI data were analyzed using MASS and FLOW (Leiden University Medical Center, Leiden, the Netherlands).

VAT and aSAT were quantified as the mean area on three transverse images at the level of the fifth lumbar vertebra. Such cross-sectional single-slice areas strongly correlate with the total VAT and aSAT volumes (38). We estimated the TBF percentage using the Tanita bio-impedance balance (TBF-310; Tanita International Division, Yiewsley, United Kingdom). Lean body mass was calculated from body weight and TBF percentage.

LV mass was evaluated in the end-diastolic phase. LV stroke volume was defined as the difference between end-diastolic volume and end-systolic volume. Similarly to several previous studies, LV mass and volumes were adjusted for lean body mass (9,39,40). LV concentricity was defined as the LV mass-to-volume ratio. We calculated the LV ejection fraction by dividing stroke volume by end-diastolic volume, multiplied by 100%, and cardiac output by multiplying stroke volume by heart rate. Diastolic function was assessed using the ratio of the mitral early and late peak filling rate (E/A ratio). We examined the aortic pulse wave velocity (PWV), as a measure of aortic stiffness, for the total aorta and regionally for the aortic arch and descending aorta. Details on the image acquisition are provided as **Supplementary Material**.

Statistical analyses

In the NEO study, individuals with a BMI of 27 kg/m^2 or higher were oversampled. For a correct representation of the associations in the general population, individuals were weighted toward the BMI distribution of participants from the Leiderdorp municipality, whose BMI distribution was similar to the BMI distribution of the Dutch general population, to adjust for the oversampling of individuals with a BMI of 27 kg/m^2 or higher (34).

Baseline characteristics were expressed as mean and standard deviation (SD), median and interquartile range, or percentage. We performed standardized linear regression analysis to assess the associations of VAT, aSAT, TBF and HOMA-IR with cardiovascular parameters. We used the standard deviation of the adiposity parameters and the normally-distributed log-transform of HOMA-IR. Regression coefficients were calculated for the total population and for men and women separately. Sex interaction was examined by assessment of the sex interaction coefficients. Similarly to others (9), we assessed the relation of insulin resistance and adipose tissue to LV mass and dimensions by adjusting for lean body mass, which is a stronger correlate for cardiac structure than body surface area or height$^{2.7}$ (39,40).

In the first model, the standardized linear regression coefficients with 95% confidence intervals (95%CI) for the associations between adiposity and cardiovascular parameters were calculated with adjustment for the potential confounding factors age, sex, ethnicity, education, smoking, physical activity, use of hormones and menopause, in addition to hypertension and lean body mass. As adiposity parameters are highly correlated (41), the first model was additionally adjusted for either VAT or TBF. The coefficients of VAT were adjusted for TBF and vice versa, as VAT is closely related to overall obesity. The coefficients of aSAT were adjusted for VAT, as the abdominal fat depots are strongly associated. In contrast, the coefficients of aSAT were not adjusted for TBF, as in general TBF mainly consists of subcutaneous fat.

In the second model, the mediating role of insulin resistance in the association between adiposity and cardiovascular parameters was evaluated, by adding HOMA-IR to the first model, after assessment of the mediator conditions (42,43). First, we evaluated the independent association between HOMA-IR and cardiovascular parameters, by adjusting for adiposity (VAT and TBF), age, sex, ethnicity, education, smoking, physical activity, use of hormones, menopause, hypertension and lean body mass. Second, we calculated the interaction coefficients between adipose tissue (VAT, aSAT and TBF) and HOMA-IR to rule out exposure-mediator interaction, whereas the relations between the fat depots and insulin resistance were confirmed previously (44). Third, we assessed the mediating role of HOMA-IR by visual inspection of the change in regression coefficient of the adiposity parameter after adding HOMA-IR to the model. Mediation by HOMA-IR was supported if the regression coefficient was fully or partly attenuated towards the null. ***P*** values <0.05 were considered to indicate significant interaction. Stata Statistical Software (release 14; StataCorp, College Station, TX) was used for the statistical analyses.

RESULTS

Baseline characteristics

In total, 6,671 participants were included in the NEO study. Cardiac MRI was acquired in a subsample of 1,207 participants. Data on both systolic and diastolic function and aortic PWV were available in 1,163 individuals. After exclusion of n=87 participants due to technical errors in systolic and/or diastolic cardiac MRI and/or aortic PWV (n=48 for systolic cardiac MRI, n=20 for diastolic cardiac MRI, n=22 for aortic PWV), consecutively n=59 because of use of glucose-lowering medication, n=65 because of a history of cardiac disease and n=38 due to missing data, the total number of participants was 914.

Table 1. Demographic, clinical and biochemical characteristics by BMI categories

	Normal weight BMI < 25 kg/m²	Overweight BMI 25-30 kg/m²	Obese BMI ≥ 30 kg/m²
Proportion of study population	42%	45%	13%
Demographic			
Age, y	55 (4)	55 (6)	56 (11)
Sex, % men	34	58	46
Ethnicity, % white	98	96	94
Education, % high	55	45	32
Median physical activity, hours/week	37.6 (16.5, 57.8)	30.2 (18.3, 47.3)	28.0 (13.3, 46.0)
Clinical			
Postmenopausal, % (women)	58	58	64
Current use of hormones, % (women)	8	12	5
Tobacco smoking, %			
Current smoker	10	14	14
Ever smoker	40	45	52
Never smoker	50	41	34
Heart rate, bpm	63 (5)	64 (11)	67 (18)
Systolic blood pressure, mmHg	129 (11)	131 (17)	135 (30)
Diastolic blood pressure, mmHg	82 (6)	85 (11)	87 (18)
Use of antihypertensive drugs, %	12	19	33
Hypertension, %	39	46	64
Use of lipid-lowering medication, %	3	9	13
Biochemical			
Fasting glucose, mmol/L	5.1 (0.3)	5.5 (0.9)	5.8 (1.5)
HbA1c, %	5.2 (0.1)	5.3 (0.4)	5.5 (0.8)
Median fasting insulin, mU/L	6.0 (4.4, 9.0)	8.9 (6.0, 12.8)	14.1 (9.9, 20.7)
Median HOMA-IR, units	1.4 (1.0, 2.1)	2.1 (1.4, 3.1)	3.4 (2.4, 5.2)
Fasting triglycerides, mg/dL	1.0 (0.3)	1.4 (0.8)	1.7 (1.8)

Table 1. Demographic, clinical and biochemical characteristics by BMI categories

	Normal weight BMI < 25 kg/m²	Overweight BMI 25-30 kg/m²	Obese BMI ≥ 30 kg/m²
Fasting total cholesterol, mmol/L	5.7 (0.5)	5.8 (1.1)	5.7 (1.9)
Fasting HDL cholesterol, mmol/L	1.7 (0.2)	1.5 (0.4)	1.3 (0.6)
Fasting LDL cholesterol, mmol/L	3.5 (0.5)	3.7 (1.0)	3.6 (1.7)

Data are means (SD) or medians (interquartile ranges). Results are based on analyses weighted toward the BMI distribution of the general population (n=914). Please note that the absolute number of individuals in each BMI category is not provided because of the weighted analysis. Abbreviations: HbA1c: glycated hemoglobin, HOMA-IR: homeostatic model assessment of insulin resistance. Due to missing values, for heart rate: n=904, HbA1c: n=910.

The study population (46% men) had a mean age (SD) of 55 (6) years, BMI of 25.9 (3.9) kg/m^2, VAT of 113 (58) cm^2 (men) and 67 (40) cm^2 (women), aSAT: 208 (77) cm^2 (men) and 260 (98) cm^2 (women), TBF: 25 (5)% (men) and 36 (6)% (women), LV mass: 96 (25) g, LV end-diastolic volume: 148 (32) mL, LV concentricity: 0.66 (0.13), LV ejection fraction: 64 (6)%, E/A ratio: 1.33 (0.46), aortic PWV: 6.6 (1.4) m/s, cardiac output: 6.2 (1.4) L/min and HOMA-IR: 2.4 (2.0). Baseline characteristics stratified by BMI are shown in **Table 1 and 2**. In contrast to aortic arch PWV, which was obtained in all participants (n=914), total aortic PWV and descending aortic PWV was available in 911 and 832 participants, respectively. Baseline characteristics of the excluded participants were similar to those of the included study population (43% men, mean age (SD): 56 (6), BMI: 26.4 (4.6) kg/m^2).

Table 2. Adiposity and cardiovascular characteristics by BMI categories

	Normal weight BMI < 25 kg/m²	Overweight BMI 25-30 kg/m²	Obese BMI ≥ 30 kg/m²
Adiposity			
Median BMI, kg/m^2	22.6 (21.5, 23.8)	26.8 (25.8, 27.9)	32.3 (31.0, 34.5)
Waist circumference, cm			
Men	89 (3)	99 (6)	113 (12)
Women	77 (3)	91 (8)	105 (15)
Hip circumference, cm			
Men	98 (2)	105 (4)	113 (10)
Women	96 (3)	106 (5)	118 (14)
Waist/hip ratio			
Men	0.90 (0.02)	0.94 (0.05)	1.00 (0.09)
Women	0.81 (0.03)	0.86 (0.06)	0.90 (0.11)
Body weight, kg			
Men	75.9 (4.3)	88.5 (8.0)	106.4 (17.7)
Women	62.2 (3.2)	75.0 (7.8)	92.0 (18.0)

Table 2. Adiposity and cardiovascular characteristics by BMI categories

	Normal weight BMI < 25 kg/m²	Overweight BMI 25-30 kg/m²	Obese BMI ≥ 30 kg/m²
Lean body mass, kg			
Men	61.0 (3.4)	65.8 (5.7)	71.2 (12.5)
Women	42.0 (1.4)	45.5 (3.2)	49.6 (6.4)
TBF, %			
Men	20 (2)	26 (3)	33 (8)
Women	32 (2)	39 (4)	46 (6)
VAT, cm^2			
Men	75 (17)	120 (50)	178 (109)
Women	45 (13)	77 (33)	128 (90)
aSAT, cm^2			
Men	155 (20)	210 (52)	331 (142)
Women	193 (30)	294 (56)	435 (170)
Cardiovascular MRI			
LV end-diastolic volume, mL	138 (16)	154 (33)	160 (59)
LV end-systolic volume, mL	50 (7)	56 (17)	60 (31)
LV mass, g	88 (11)	101 (26)	104 (54)
LV concentricity, g/mL	0.65 (0.06)	0.66 (0.14)	0.66 (0.26)
LV ejection fraction, %	64 (3)	64 (6)	63 (11)
E/A ratio	1.39 (0.25)	1.31 (0.50)	1.17 (0.61)
LV stroke volume, mL	88 (10)	98 (22)	100 (37)
LV cardiac output, L	5.9 (0.7)	6.4 (1.4)	6.7 (2.6)
Aortic PWV, m/s			
Total aorta	6.7 (0.9)	6.6 (1.2)	6.7 (2.1)
Aortic arch	6.5 (1.1)	6.6 (2.3)	6.8 (4.0)
Descending aorta	7.0 (1.3)	6.8 (1.8)	6.9 (2.9)

Data are means (SD) or medians (interquartile ranges). Abbreviations: aSAT: abdominal subcutaneous adipose tissue, E/A ratio: ratio of mitral early and late peak filling rate, LV: left ventricular, LV concentricity: LV mass-to-volume ratio, PWV: pulse wave velocity, TBF: total body fat, VAT: visceral adipose tissue. Results are based on analyses weighted toward the BMI distribution of the general population (n=914). Due to missing values, for PWV total aorta: n=911, PWV descending aorta: n=832.

Adiposity and cardiovascular parameters

The regression coefficients for the relation of adiposity to cardiovascular parameters, in the total population and in men and women separately are presented in **Supplemental Table 1** and **Table 3**, respectively. In the total population (**Supplemental Table 1**), VAT as compared with TBF was differently associated with most of the cardiovascular parameters, except for LV diastolic function. In general, the associations between aSAT and the cardiovascular parameters were weaker than for VAT and TBF. VAT was associated with a smaller LV end-diastolic volume (-8.9 (-11.7;-6.1) mL per SD VAT) and reduced stroke volume and cardiac output, whereas for TBF those parameters were higher (LV end-diastolic volume: +5.4 (1.1;9.7) mL per SD TBF). There were no associations between aSAT and LV end-diastolic volume and cardiac output.

For VAT, the reduction in LV end-diastolic volume was paralleled by a small decrease in LV mass (-3.3 (-5.1;-1.6) g per SD VAT) and therefore, LV concentricity was slightly higher (+0.02 (0.00;0.03) per SD VAT). For TBF, the increase in LV end-diastolic volume was larger than the slight increase in LV mass (+0.6 (-1.7;2.9) g/mL per SD TBF). As a result, TBF was associated with a slightly lower LV concentricity (-0.02 (-0.04;0.00) g/mL per SD TBF). Results were generally similar in the analyses with indexing to height$^{2.7}$ instead of adjusting for lean body mass (**Supplemental Table 2**).

The aSAT- and TBF-related changes in LV end-diastolic volume and/or stroke volume resulted in small changes in LV ejection fraction. Of importance, all fat parameters were or tended to be associated with a small reduction in E/A ratio: -0.04 (-0.09;0.01) per SD VAT; -0.05 (-0.10;0.00) per SD aSAT; -0.09 (-0.16;-0.02) per SD TBF. In the total population, the regression coefficients for the associations between the adiposity parameters and total and regional aortic PWV were all around zero.

Sex differences were present in the association of TBF and aSAT with LV mass and LV concentricity and in the relation of adiposity to aortic arch PWV (**Table 3** and **Figure 2**). TBF tended to be related to a higher LV mass in men, but not in women (***P*** interaction=0.04), and aSAT was associated with a lower LV mass in women, but not in men (***P*** interaction=0.01). As a result, the differential relation of VAT versus TBF and aSAT with LV concentricity (higher versus lower LV concentricity, respectively) was more pronounced in women than in men. Furthermore, VAT, aSAT and TBF were associated with a higher aortic arch PWV in women, but not in men (***P*** interaction=0.001, 0.048 and 0006, respectively).

Table 3. Associations of HOMA-IR, VAT, aSAT and TBF with cardiovascular parameters, stratified by sex

	Adjusted standardized difference in cardiovascular parameters (95%CI)		
	Men (46%)	**Women (54%)**	***P* interaction**
LV structure			
LV mass, g			
Log HOMA-IR	-3.6 (-7.2 to 0.1)	-5.0 (-7.9 to -2.1)	0.09
VAT (SD: 54 cm^2)	-3.4 (-5.7 to -1.2)	-4.2 (-7.2 to -1.2)	0.06
aSAT (SD: 94 cm^2)	0.2 (-2.3 to 2.8)	-4.0 (-6.0 to -2.0)	0.01
TBF (SD: 8%)	2.6 (-1.4 to 6.5)	0.6 (-2.3 to 3.7)	0.04
LV end-diastolic volume, mL			
Log HOMA-IR	-10.5 (-15.2 to -5.9)	-6.4 (-10.4 to -2.5)	0.6
VAT (SD: 54 cm^2)	-7.6 (-11.3 to -3.9)	-11.1 (-15.1 to -7.1)	0.2
aSAT (SD: 94 cm^2)	2.5 (-1.7 to 6.6)	-3.0 (-6.2 to 0.2)	0.3
TBF (SD: 8%)	6.4 (0.1 to 12.7)	4.3 (-2.3 to 10.9)	0.4
LV concentricity, g/mL			
Log HOMA-IR	0.03 (0.00 to 0.05)	-0.01 (-0.03 to 0.01)	0.02
VAT (SD: 54 cm^2)	0.01 (-0.01 to 0.03)	0.02 (0.00 to 0.05)	0.8
aSAT (SD: 94 cm^2)	-0.01 (-0.03 to 0.01)	-0.02 (-0.03 to 0.00)	0.4
TBF (SD: 8%)	-0.01 (-0.04 to 0.02)	-0.02 (-0.05 to 0.01)	0.4
LV function			
LV ejection fraction, %			
Log HOMA-IR	0.7 (-0.5 to 1.8)	-0.5 (-1.5 to 0.5)	0.3
VAT (SD: 54 cm^2)	0.4 (-0.5 to 1.2)	-0.3 (-1.4 to 0.8)	0.7
aSAT (SD: 94 cm^2)	-0.3 (-1.2 to 0.6)	-0.9 (-1.7 to -0.2)	0.5
TBF (SD: 8%)	-1.3 (-2.6 to 0.0)	-0.4 (-1.5 to 0.6)	0.6
E/A ratio			
Log HOMA-IR	-0.17 (-0.27 to -0.07)	-0.04 (-0.12 to 0.03)	0.2
VAT (SD: 54 cm^2)	-0.01 (-0.08 to 0.06)	-0.09 (-0.16 to -0.02)	0.3
aSAT (SD: 94 cm^2)	-0.06 (-0.13 to 0.00)	-0.04 (-0.11 to 0.04)	0.7
TBF (SD: 8%)	-0.12 (-0.22 to -0.02)	-0.07 (-0.18 to 0.05)	0.8
Aortic stiffness			
Total aorta, m/s			
Log HOMA-IR	0.1 (-0.1 to 0.4)	-0.1 (-0.3 to 0.2)	0.9
VAT (SD: 54 cm^2)	-0.1 (-0.2 to 0.1)	0.1 (-0.2 to 0.4)	0.3
aSAT (SD: 94 cm^2)	0.1 (-0.1 to 0.3)	-0.1 (-0.3 to 0.1)	0.6
TBF (SD: 8%)	0.1 (-0.2 to 0.3)	-0.1 (-0.4 to 0.2)	0.7

Table 3. Associations of HOMA-IR, VAT, aSAT and TBF with cardiovascular parameters, stratified by sex

	Adjusted standardized difference in cardiovascular parameters (95%CI)		
	Men (46%)	**Women (54%)**	***P* interaction**
Aortic arch, m/s			
Log HOMA-IR	0.0 (-0.5 to 0.5)	-0.1 (-0.6 to 0.3)	0.3
VAT (SD: 54 cm^2)	-0.1 (-0.5 to 0.2)	0.3 (0.0 to 0.6)	0.001
aSAT (SD: 94 cm^2)	0.0 (-0.3 to 0.3)	0.1 (-0.1 to 0.4)	0.048
TBF (SD: 8%)	0.0 (-0.5 to 0.5)	0.3 (0.0 to 0.7)	0.006
Descending aorta, m/s			
Log HOMA-IR	0.2 (-0.1 to 0.6)	-0.2 (-0.5 to 0.2)	0.3
VAT (SD: 54 cm^2)	-0.1 (-0.3 to 0.1)	0.0 (-0.5 to 0.6)	0.8
aSAT (SD: 94 cm^2)	0.1 (-0.1 to 0.4)	-0.2 (-0.5 to 0.1)	0.1
TBF (SD: 8%)	0.1 (-0.2 to 0.4)	-0.2 (-0.7 to 0.3)	0.5
Hemodynamics			
Stroke volume, mL			
Log HOMA-IR	-5.3 (-8.7 to -1.9)	-4.6 (-7.3 to -1.9)	0.9
VAT (SD: 54 cm^2)	-4.3 (-6.8 to -1.9)	-7.5 (-10.2 to -4.8)	0.2
aSAT (SD: 94 cm^2)	0.9 (-1.9 to 3.7)	-3.4 (-5.4 to -1.3)	0.3
TBF (SD: 8%)	2.0 (-2.2 to 6.1)	1.9 (-2.2 to 6.1)	0.7
Cardiac output, mL			
Log HOMA-IR	181 (-76 to 438)	-144 (-371 to 84)	0.2
VAT (SD: 54 cm^2)	-126 (-308 to 56)	-321 (-519 to -122)	0.9
aSAT (SD: 94 cm^2)	71 (-126 to 267)	-128 (-280 to 23)	1.0
TBF (SD: 8%)	125 (-158 to 407)	264 (-10 to 537)	0.4

Results represent regression coefficients per 10-fold increase in HOMA-IR or per SD of measure of adiposity and are corrected for age, ethnicity, education, smoking, physical activity, use of hormone therapy, menopausal state, hypertension, lean body mass and adiposity (HOMA-IR is adjusted for VAT and TBF, VAT is adjusted for TBF, and aSAT and TBF are adjusted for VAT). ***P*** values for interaction by sex. Abbreviations: aSAT: abdominal subcutaneous adipose tissue, E/A ratio: ratio of mitral early and late peak filling rate, log HOMA-IR: log-transformation of the homeostatic model assessment of insulin resistance, LV: left ventricular, LV concentricity: LV mass-to-volume ratio, PWV: pulse wave velocity, TBF: total body fat, VAT: visceral adipose tissue. Results are based on analyses weighted toward the BMI distribution of the general population (n=914). Due to missing values, for PWV total aorta: n=911, PWV descending aorta: n=832.

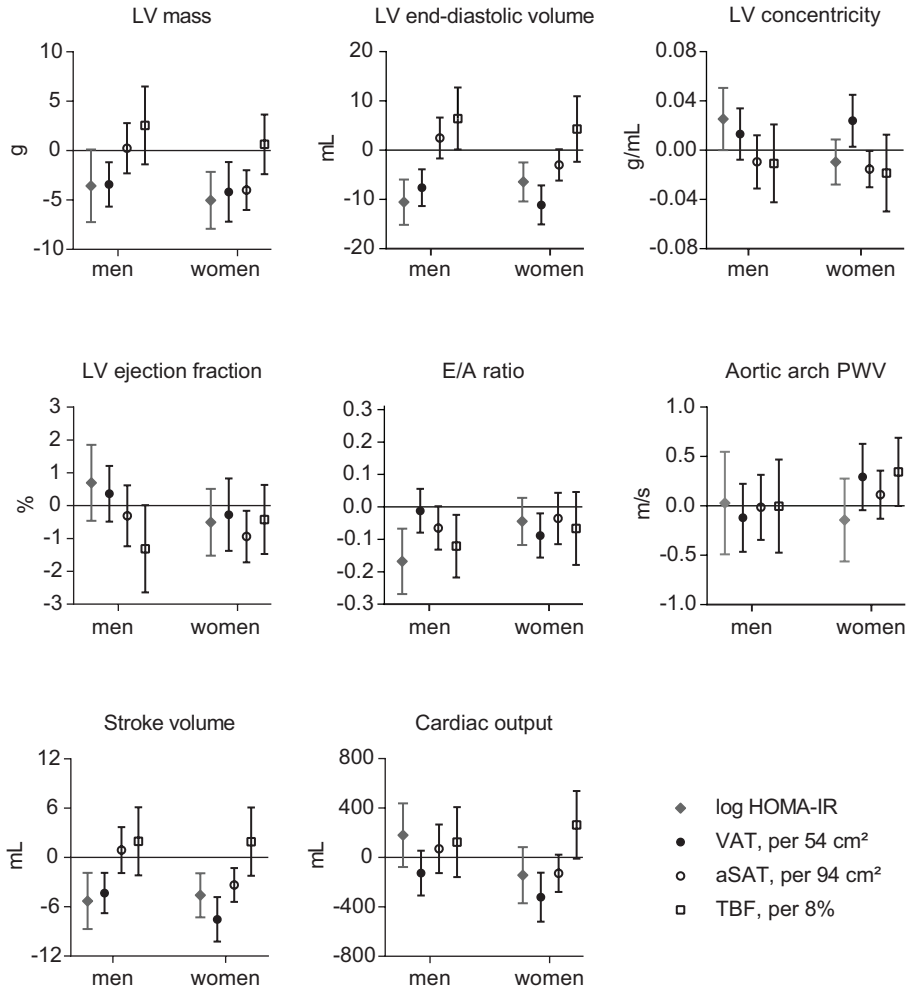

Figure 2. Associations of HOMA-IR, VAT, aSAT and TBF with cardiovascular parameters for men and women. Adjusted standardized regression coefficients (95%CI) in men and women for the association of HOMA-IR (log-transformation) (=***solid diamond***), VAT (SD: 54 cm^2) (=***solid circle***), aSAT (SD: 94 cm^2) (=***open circle***) and TBF (SD: 8%) (=***open square***) with cardiovascular parameters (after adjustment for potential confounding factors, see Table 3). Abbreviations: aSAT: abdominal subcutaneous adipose tissue, E/A ratio: ratio of mitral early and late peak filling rate, HOMA-IR: homeostatic model assessment of insulin resistance, LV: left ventricular, LV concentricity: LV mass-to-volume ratio, PWV: pulse wave velocity, TBF: total body fat, VAT: visceral adipose tissue.

Table 4. Mediating role of HOMA-IR in the associations of VAT, aSAT and TBF with cardiovascular parameters

	Adjusted standardized difference in cardiovascular parameters (95%CI	
	Model 1: adjusted for confounding factors	**Model 2: model 1 + adjusted for insulin resistance**
LV end-diastolic volume, mL		
VAT (SD: 54 cm^2)	-8.9 (-11.7 to -6.1)	-7.0 (-9.7 to -4.3)
aSAT (SD: 94 cm^2)	-0.5 (-2.9 to 1.8)	0.4 (-1.8 to 2.7)
TBF (SD: 8%)	5.4 (1.1 to 9.7)	7.5 (3.1 to 11.9)
Stroke volume, mL		
VAT (SD: 54 cm^2)	-5.6 (-7.5 to -3.7)	-4.4 (-6.2 to -2.6)
aSAT (SD: 94 cm^2)	-1.4 (-2.9 to 0.2)	-0.8 (-2.4 to 0.8)
TBF (SD: 8%)	2.2 (-0.5 to 4.9)	3.5 (0.6 to 6.3)
E/A ratio		
VAT (SD: 54 cm^2)	-0.04 (-0.09 to 0.01)	-0.02 (-0.07 to 0.04)
aSAT (SD: 94 cm^2)	-0.05 (-0.10 to 0.00)	-0.03 (-0.08 to 0.02)
TBF (SD: 8%)	-0.09 (-0.16 to -0.02)	-0.06 (-0.13 to 0.01)

Results represent regression coefficients per SD of measure of adiposity. Model 1: adjusted for age, sex, ethnicity, education, smoking, physical activity, use of hormone therapy, menopausal state, hypertension, lean body mass and adiposity (VAT is adjusted for TBF, and aSAT and TBF are adjusted for VAT). Model 2: model 1 + adjusted for HOMA-IR. For abbreviations, see Table 3.

Mediating role of insulin resistance

In the total population (**Supplemental Table 1**), HOMA-IR was associated with a lower E/A ratio and smaller LV end-diastolic volume (-0.11 (-0.17;-0.05) and -8.5 (-11.5;-5.5) mL per 10-fold increase in HOMA-IR, respectively), paralleled by a reduction in LV mass, a slightly higher LV concentricity, and a reduced stroke volume. Results were similar when indexing to $height^{2.7}$ instead of accounting for lean body mass (**Supplemental Table 2**). In contrast, HOMA-IR was not associated with LV ejection fraction, cardiac output or aortic PWV. In the analyses stratified by sex (**Table 3** and **Figure 2**), HOMA-IR was associated with a higher LV concentricity in men, but not in women (***P*** interaction=0.02).

As HOMA-IR appeared to be related to a lower E/A ratio and smaller LV dimensions, similarly in men and women, HOMA-IR was included as a mediating variable in the models on the association of adiposity with E/A ratio, LV end-diastolic volume and stroke volume, after ruling out exposure-mediator interaction (***P*** interaction >0.2 for all associations). As shown in **Table 4** and **Figure 3**, HOMA-IR attenuated the association between the fat depots and E/A ratio, and between VAT and LV end-diastolic volume and stroke volume.

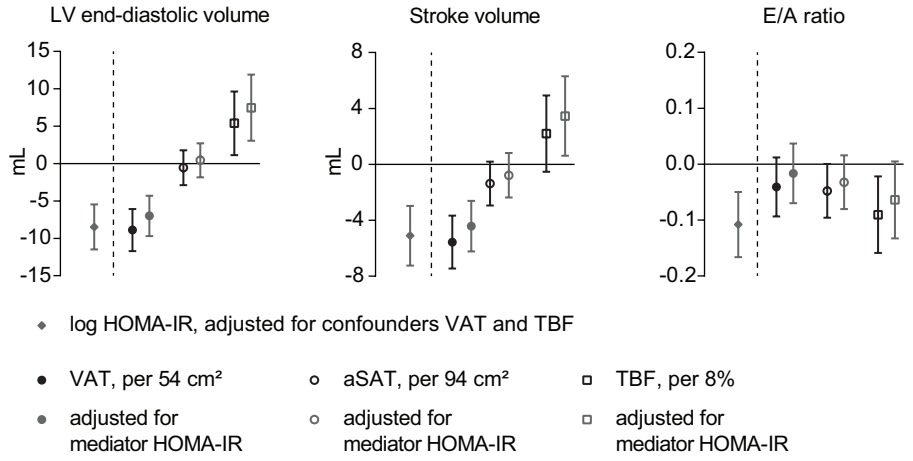

Figure 3. Mediating role of HOMA-IR in the associations of VAT, aSAT and TBF with cardiovascular parameters. Adjusted standardized regression coefficients (95%CI) in the total population for the association of HOMA-IR (log-transformation) (=***solid diamond***) and VAT (SD: 54 cm^2) (=***solid circle***), aSAT (SD: 94 cm^2) (=***open circle***) and TBF (SD: 8%) (=***open square***) with cardiovascular parameters. Regression coefficients for adiposity are presented after adjustment for potential confounding factors (model 1, see Table 4) (***each left bar, in black***) and after adding HOMA-IR as a mediator to the model (model 2, see Table 4) (***each right bar, in gray***). For abbreviations, see Figure 2.

DISCUSSION

In previous studies, the separate effects of insulin resistance, visceral and subcutaneous fat in obesity-related cardiovascular remodeling have not been fully disentangled. In this population-based study including middle-aged men and women without use of glucose-lowering medication and no history of cardiovascular disease, insulin resistance was associated with a lower diastolic function, independently of VAT and TBF; in contrast, insulin resistance was not associated with systolic function and aortic stiffness. Furthermore, insulin resistance partly mediated the relations of VAT, aSAT and TBF to reduced diastolic function as well as the relationship of VAT to a smaller LV end-diastolic volume. Interestingly, all fat depots were associated with a lower diastolic function, while VAT and TBF demonstrated distinct associations with LV dimensions. In this population-based study, the differential association between VAT versus TBF fat with LV structure and dimensions (higher versus lower LV concentricity, respectively) was more pronounced in women than in men, and all adiposity parameters were associated with a higher aortic arch PWV in women, but not in men.

Insulin resistance

Our results expand current literature on the relation of insulin resistance, abnormal glucose metabolism and type 2 diabetes to diastolic dysfunction (17,18,32,33,45). Several large-scale

studies have described reduced diastolic function in association with abnormalities in glucose regulation; for example, the Strong Heart Study reported a lower Doppler E/A ratio in non-diabetic, non-hypertensive individuals with impaired fasting glucose and/or impaired glucose tolerance than in those with normal glucose tolerance (17), and the ARIC (Atherosclerosis Risk In the Community) study demonstrated higher echocardiography-derived LV filling pressures associated with glycemic status (normal, prediabetes or type 2 diabetes), independent of BMI (18). Whereas BMI is less complex, expensive and time consuming than direct adipose tissue measures, it is an inaccurate metric of excess body fat and visceral adiposity (46). Therefore, the cardiovascular effects of insulin resistance and VAT might not be fully disentangled by adjustment for BMI. Importantly, this study confirms the relation of insulin resistance to reduced diastolic function in the middle-aged general population, separately from VAT and TBF. Also, our study allows for the appreciation of the relative contribution of insulin resistance, in comparison with adipose tissue, to impairments in diastolic function.

Unlike the findings of previous population-based studies (7,8,17-21,29-31), in our study, insulin resistance was not associated with increased cardiac mass but neither was adiposity, which might be attributable to the lower degree of obesity in our population (BMI of ~25.9 kg/m2). Interestingly, several population-based studies have reported an increasing LV mass with worsening abnormalities in glucose metabolism, particularly in women (18,19,47,48). In view of these previous findings, our observation of a higher LV concentricity with increasing HOMA-IR in men, but not in women, is remarkable. However, it should be noted that this HOMA-IR-related increase in LV concentricity in men was without an increase in LV mass. Also, we did not observe sex differences in the associations of HOMA-IR with LV end-diastolic volume and LV mass, which prevents us from drawing definitive conclusions regarding sex-related differences in the impact of HOMA-IR on LV concentric remodeling.

Proposed mechanisms for reduced diastolic function in insulin-resistant individuals comprise abnormalities in myocardial energetics and calcium homeostasis (25,26,49). Interestingly, the contribution of metabolic processes to impairments in diastolic function may be larger as compared with LV geometric remodeling (25). Insulin resistance has been shown to alter the myocardial substrate preference, which is associated with adenosine triphosphate (ATP) shortage (23,24). Diastolic rather than systolic function has been demonstrated to be primarily affected by energy shortage (26). Additionally, altered myocardial tissue characteristics, including collagen deposition and triglyceride accumulation, may increase myocardial stiffness and contribute to impaired LV relaxation (50,51), although the association between insulin resistance and impaired diastolic function has been shown to be independent of myocardial fibrosis (52). In our study, insulin resistance and VAT were also associated with a smaller LV end-diastolic volume. Interestingly, a recent study in type 2 diabetes patients described a link between cardiac steatosis and phosphocreatine (PCr)-to-ATP ratios and concentric LV remodeling, suggesting a role for myocardial lipotoxicity and energetic status in type 2 diabetes-related LV morphologic changes (51).

Adipose tissue

The various fat depots were differently associated with LV dimensions and hemodynamics. TBF was related to a higher cardiac output, presumably due to increased metabolic demands (53), whereas VAT was associated with lower blood flow rates. This divergent association of VAT and SAT with LV morphology and hemodynamic parameters is in keeping with the UK Biobank data (14), the Dallas Heart Study (9) and the MESA (Multi-Ethnic Study of Atherosclerosis) (29,30). VAT in particular may attract macrophages and this chronic low-grade inflammatory state may cause endothelial dysfunction (11). In our study, VAT was associated with a smaller LV end-diastolic volume and higher LV concentricity, particularly in women. Accordingly, it has been previously shown that cardiac adaptations to obesity are more severe in women, which might be attributable to sex differences in biological factors associated with adipose tissue (54).

Interestingly, in the UK Biobank study (14), women showed a stronger relation of VAT to increased total vascular stiffness as compared with men. In our study, adiposity-related aortic arch stiffening was present in women, but not in men. In addition to hyperleptinemia, increased circulating inflammatory markers and local inflammation of perivascular fat (8,55), in some studies, insulin resistance has been implicated in obesity-related aortic stiffening (56,57); however, a mediating role of HOMA-IR in the relation of adiposity to increased aortic stiffness was not supported by our data. While age- and hypertension-related aortic stiffening is thought to be due to progressive declines in elastin primarily in the proximal aorta (58), the mechanisms by which adiposity might impair total and regional vascular function remain to be elucidated and in particular the impact of sex may warrant further research.

Implications

In our population, the observed reductions in diastolic function were small, as MRI-derived E/A ratio values in normal diastolic function range from 0.8 to 1.5 (59). Also, insulin resistance did not completely mediate the associations between adipose tissue and reduced diastolic function, which implies that other factors including inflammation, increased leptin and autonomic dysfunction are likely to may play a role in the pathogenesis of diastolic dysfunction in obesity (60,61). Nonetheless, the results of this study confirm that insulin resistance, separate from adipose tissue, is associated with reduced diastolic function, thereby supporting that diastolic dysfunction is indeed a characteristic of diabetic cardiomyopathy. Furthermore, concentric remodeling has been associated with an increased susceptibility of heart failure events (62). In this context, our results reaffirm the clinical importance of differentiating visceral and subcutaneous adiposity, as VAT but not TBF was associated with a smaller LV end-diastolic volume.

Limitations

Some limitations need to be addressed. The cross-sectional design does not allow to draw conclusions on causality, neither on the direction of the associations. Also, our study may not

have sufficient power to draw conclusions on sex differences in obesity-related cardiovascular remodeling, as the observed changes in cardiovascular parameters related to adiposity and insulin resistance were small. We excluded individuals using type 2 diabetes medication, who may have the largest impairments in diastolic function, because glucose-lowering drugs may influence insulin resistance or modify the relation of insulin resistance to cardiovascular parameters (37). Furthermore, we used HOMA-IR as a feasible alternative for the hyperinsulinemic euglycemic clamp, which is considered the gold standard for whole-body insulin resistance. HOMA-IR is widely used in epidemiologic studies and corresponds well to estimates of insulin resistance in clamp studies (63). Interestingly, advanced PET/MR protocols which enable the measurement of tissue-specific insulin sensitivity may help to gain more insight into the association of myocardial insulin resistance with cardiac remodeling (64). In the NEO study, diastolic function is derived from MRI. MRI values for the E/A ratio are highly reproducible and strongly correlate with echocardiography measurements (65-67). However, in clinical patients, the diagnosis of diastolic dysfunction is based on echocardiography, using multiple diastolic function parameters, in combination with the evaluation for signs or symptoms of congestive heart failure (68). For example, we did not have data on left atrial size, which can be used as a measure of chronic diastolic dysfunction. Furthermore, we examined LV ejection fraction, whereas systolic strain is considered a more sensitive measure for LV contractility (18,20). Accordingly, in the Strong Heart Study, insulin resistance was related to lower systolic strain and reduced measures of myocardial mechano-energetic efficiency, whereas LV ejection fraction was unaltered (69).

CONCLUSION

In this cross-sectional population-based imaging study in middle-aged men and women, we document that insulin resistance has a mediating role in the relation between adipose tissue and a lower E/A ratio and between VAT and a smaller LV end-diastolic volume. All fat depots including VAT, aSAT and TBF were related to reduced diastolic function, whereas VAT but not TBF was associated with smaller LV dimensions. We assessed specific adiposity metrics rather than excess body weight. The present study demonstrates that insulin resistance is associated with a lower E/A ratio and a smaller LV end-diastolic volume, separately from VAT and TBF, supporting reduced diastolic function and smaller LV dimensions as adiposity-independent characteristics of insulin resistance-related cardiovascular remodeling, in the middle-aged general population.

ACKNOWLEDGEMENTS

We express our gratitude to all individuals who participate in the Netherlands Epidemiology of Obesity (NEO) study. We are grateful to all participating general practitioners for inviting eligible participants. We furthermore thank P.R. van Beelen and all research nurses for data collection, P.J. Noordijk and her team for sample handling and storage, and I. de Jonge for data management.

FUNDING

This project was funded by the 'Cardio Vascular Imaging Group (CVIG)', Leiden University Medical Center (Leiden, the Netherlands). The NEO study is supported by the participating Departments, the Division and the Board of Directors of the Leiden University Medical Center, and by the Leiden University, Research Profile Area 'Vascular and Regenerative Medicine'.

REFERENCES

1. Seferovic PM, Paulus WJ. Clinical diabetic cardiomyopathy: a two-faced disease with restrictive and dilated phenotypes. Eur Heart J 2015;36(27):1718-1727, 1727a-1727c.
2. Rubler S, Dlugash J, Yuceoglu YZ, Kumral T, Branwood AW, Grishman A. New type of cardiomyopathy associated with diabetic glomerulosclerosis. Am J Cardiol 1972;30(6):595-602.
3. Richardson P, McKenna W, Bristow M, et al. Report of the 1995 World Health Organization/ International Society and Federation of Cardiology Task Force on the Definition and Classification of cardiomyopathies. Circulation 1996;93(5):841-842.
4. Mokdad AH, Ford ES, Bowman BA, et al. Prevalence of obesity, diabetes, and obesity-related health risk factors, 2001. JAMA 2003;289(1):76-79.
5. Lauer MS, Anderson KM, Kannel WB, Levy D. The impact of obesity on left ventricular mass and geometry. The Framingham Heart Study. JAMA 1991;266(2):231-236.
6. Heckbert SR, Post W, Pearson GD, et al. Traditional cardiovascular risk factors in relation to left ventricular mass, volume, and systolic function by cardiac magnetic resonance imaging: the Multiethnic Study of Atherosclerosis. J Am Coll Cardiol 2006;48(11):2285-2292.
7. Brunner EJ, Shipley MJ, Ahmadi-Abhari S, et al. Adiposity, obesity, and arterial aging: longitudinal study of aortic stiffness in the Whitehall II cohort. Hypertension 2015;66(2):294-300.
8. Britton KA, Wang N, Palmisano J, et al. Thoracic periaortic and visceral adipose tissue and their cross-sectional associations with measures of vascular function. Obesity (Silver Spring) 2013;21(7):1496-1503.
9. Neeland IJ, Gupta S, Ayers CR, et al. Relation of regional fat distribution to left ventricular structure and function. Circ Cardiovasc Imaging 2013;6(5):800-807.
10. Neeland IJ, Turer AT, Ayers CR, et al. Body fat distribution and incident cardiovascular disease in obese adults. J Am Coll Cardiol 2015;65(19):2150-2151.
11. Hamdy O, Porramatikul S, Al-Ozairi E. Metabolic obesity: the paradox between visceral and subcutaneous fat. Curr Diabetes Rev 2006;2(4):367-373.
12. Ziemke F, Mantzoros CS. Adiponectin in insulin resistance: lessons from translational research. Am J Clin Nutr 2010;91(1):258S-261S.
13. Li S, Shin HJ, Ding EL, van Dam RM. Adiponectin levels and risk of type 2 diabetes: a systematic review and meta-analysis. JAMA 2009;302(2):179-188.
14. van Hout MJP, Dekkers IA, Westenberg JJM, Schalij MJ, Scholte A, Lamb HJ. The impact of visceral and general obesity on vascular and left ventricular function and geometry: a cross-sectional magnetic resonance imaging study of the UK Biobank. Eur Heart J Cardiovasc Imaging 2019.
15. Wade KH, Chiesa ST, Hughes AD, et al. Assessing the causal role of body mass index on cardiovascular health in young adults: Mendelian randomization and recall-by-genotype analyses. Circulation 2018;138(20):2187-2201.
16. Cho DH, Kim MN, Joo HJ, Shim WJ, Lim DS, Park SM. Visceral obesity, but not central obesity, is associated with cardiac remodeling in subjects with suspected metabolic syndrome. Nutr Metab Cardiovasc Dis 2019;29(4):360-366.
17. Capaldo B, Di Bonito P, Iaccarino M, et al. Cardiovascular Characteristics in Subjects With Increasing Levels of Abnormal Glucose Regulation The Strong Heart Study. Diabetes Care 2013;36(4):992-997.
18. Skali H, Shah A, Gupta DK, et al. Cardiac structure and function across the glycemic spectrum in elderly men and women free of prevalent heart disease: the Atherosclerosis Risk In the Community study. Circ Heart Fail 2015;8(3):448-454.
19. Galderisi M, Anderson KM, Wilson PW, Levy D. Echocardiographic evidence for the existence of a distinct diabetic cardiomyopathy (the Framingham Heart Study). Am J Cardiol 1991;68(1):85-89.
20. Devereux RB, Roman MJ, Paranicas M, et al. Impact of diabetes on cardiac structure and function: the strong heart study. Circulation 2000;101(19):2271-2276.
21. Bertoni AG, Goff DC, Jr., D'Agostino RB, Jr., et al. Diabetic cardiomyopathy and subclinical cardiovascular disease: the Multi-Ethnic Study of Atherosclerosis (MESA). Diabetes Care 2006;29(3):588-594.
22. Sawada N, Daimon M, Kawata T, et al. The

Significance of the Effect of Visceral Adiposity on Left Ventricular Diastolic Function in the General Population. Sci Rep 2019;9(1):4435.
23. Rider OJ, Cox P, Tyler D, Clarke K, Neubauer S. Myocardial substrate metabolism in obesity. Int J Obes (Lond) 2013;37(7):972-979.
24. Rijzewijk LJ, van der Meer RW, Lamb HJ, et al. Altered myocardial substrate metabolism and decreased diastolic function in nonischemic human diabetic cardiomyopathy: studies with cardiac positron emission tomography and magnetic resonance imaging. J Am Coll Cardiol 2009;54(16):1524-1532.
25. Rayner JJ, Banerjee R, Holloway CJ, et al. The relative contribution of metabolic and structural abnormalities to diastolic dysfunction in obesity. Int J Obes (Lond) 2018;42(3):441-447.
26. Rider OJ, Francis JM, Ali MK, et al. Effects of catecholamine stress on diastolic function and myocardial energetics in obesity. Circulation 2012;125(12):1511-1519.
27. von Bibra H, St John Sutton M. Diastolic dysfunction in diabetes and the metabolic syndrome: promising potential for diagnosis and prognosis. Diabetologia 2010;53(6):1033-1045.
28. Chinali M, de Simone G, Roman MJ, et al. Impact of obesity on cardiac geometry and function in a population of adolescents: the Strong Heart Study. J Am Coll Cardiol 2006;47(11):2267-2273.
29. Abbasi SA, Hundley WG, Bluemke DA, et al. Visceral adiposity and left ventricular remodeling: The Multi-Ethnic Study of Atherosclerosis. Nutr Metab Cardiovasc Dis 2015;25(7):667-676.
30. Shah RV, Abbasi SA, Heydari B, et al. Insulin resistance, subclinical left ventricular remodeling, and the obesity paradox: MESA (Multi-Ethnic Study of Atherosclerosis). J Am Coll Cardiol 2013;61(16):1698-1706.
31. Velagaleti RS, Gona P, Chuang ML, et al. Relations of insulin resistance and glycemic abnormalities to cardiovascular magnetic resonance measures of cardiac structure and function: the Framingham Heart Study. Circ Cardiovasc Imaging 2010;3(3):257-263.
32. Stahrenberg R, Edelmann F, Mende M, et al. Association of glucose metabolism with diastolic function along the diabetic continuum. Diabetologia 2010;53(7):1331-1340.
33. Fontes-Carvalho R, Ladeiras-Lopes R, Bettencourt P, Leite-Moreira A, Azevedo A. Diastolic dysfunction in the diabetic continuum: association with insulin resistance, metabolic syndrome and type 2 diabetes. Cardiovasc Diabetol 2015;14:4.
34. de Mutsert R, den Heijer M, Rabelink TJ, et al. The Netherlands Epidemiology of Obesity (NEO) study: study design and data collection. Eur J Epidemiol 2013;28(6):513-523.
35. Williams B, Mancia G, Spiering W, et al. 2018 ESC/ESH Guidelines for the management of arterial hypertension. Eur Heart J 2018;39(33):3021-3104.
36. Matthews DR, Hosker JP, Rudenski AS, Naylor BA, Treacher DF, Turner RC. Homeostasis model assessment: insulin resistance and beta-cell function from fasting plasma glucose and insulin concentrations in man. Diabetologia 1985;28(7):412-419.
37. Wallace TM, Levy JC, Matthews DR. Use and abuse of HOMA modeling. Diabetes Care 2004;27(6):1487-1495.
38. Schweitzer L, Geisler C, Pourhassan M, et al. What is the best reference site for a single MRI slice to assess whole-body skeletal muscle and adipose tissue volumes in healthy adults? Am J Clin Nutr 2015;102(1):58-65.
39. Bella JN, Devereux RB, Roman MJ, et al. Relations of left ventricular mass to fat-free and adipose body mass: the strong heart study. The Strong Heart Study Investigators. Circulation 1998;98(23):2538-2544.
40. Daniels SR, Kimball TR, Morrison JA, Khoury P, Witt S, Meyer RA. Effect of lean body mass, fat mass, blood pressure, and sexual maturation on left ventricular mass in children and adolescents. Statistical, biological, and clinical significance. Circulation 1995;92(11):3249-3254.
41. Seidell JC, Bouchard C. Visceral fat in relation to health: is it a major culprit or simply an innocent bystander? Int J Obes Relat Metab Disord 1997;21(8):626-631.
42. Richiardi L, Bellocco R, Zugna D. Mediation analysis in epidemiology: methods, interpretation and bias. Int J Epidemiol 2013;42(5):1511-1519.
43. Robins JM, Greenland S. Identifiability and exchangeability for direct and indirect effects. Epidemiology 1992;3(2):143-155.
44. de Mutsert R, Gast K, Widya R, et al. Associations of Abdominal Subcutaneous and Visceral Fat with Insulin Resistance and Secretion Differ Between Men and Women: The Netherlands Epidemiology of Obesity Study. Metab Syndr Relat Disord 2018;16(1):54-63.
45. From AM, Scott CG, Chen HH. The development

of heart failure in patients with diabetes mellitus and pre-clinical diastolic dysfunction a population-based study. J Am Coll Cardiol 2010;55(4):300-305.
46. Ortega FB, Lavie CJ, Blair SN. Obesity and Cardiovascular Disease. Circ Res 2016;118(11):1752-1770.
47. Rutter MK, Parise H, Benjamin EJ, et al. Impact of glucose intolerance and insulin resistance on cardiac structure and function: sex-related differences in the Framingham Heart Study. Circulation 2003;107(3):448-454.
48. Ilercil A, Devereux RB, Roman MJ, et al. Relationship of impaired glucose tolerance to left ventricular structure and function: The Strong Heart Study. Am Heart J 2001;141(6):992-998.
49. Lebeche D, Davidoff AJ, Hajjar RJ. Interplay between impaired calcium regulation and insulin signaling abnormalities in diabetic cardiomyopathy. Nat Clin Pract Cardiovasc Med 2008;5(11):715-724.
50. Wong TC, Piehler KM, Kang IA, et al. Myocardial extracellular volume fraction quantified by cardiovascular magnetic resonance is increased in diabetes and associated with mortality and incident heart failure admission. Eur Heart J 2014;35(10):657-664.
51. Levelt E, Mahmod M, Piechnik SK, et al. Relationship Between Left Ventricular Structural and Metabolic Remodeling in Type 2 Diabetes. Diabetes 2016;65(1):44-52.
52. Ladeiras-Lopes R, Moreira HT, Bettencourt N, et al. Metabolic Syndrome Is Associated With Impaired Diastolic Function Independently of MRI-Derived Myocardial Extracellular Volume: The MESA Study. Diabetes 2018;67(5):1007-1012.
53. Collis T, Devereux RB, Roman MJ, et al. Relations of stroke volume and cardiac output to body composition: the strong heart study. Circulation 2001;103(6):820-825.
54. De Simone G, Devereux RB, Chinali M, et al. Sex differences in obesity-related changes in left ventricular morphology: the Strong Heart Study. J Hypertens 2011;29(7):1431-1438.
55. Rider OJ, Tayal U, Francis JM, et al. The effect of obesity and weight loss on aortic pulse wave velocity as assessed by magnetic resonance imaging. Obesity (Silver Spring) 2010;18(12):2311-2316.
56. Webb DR, Khunti K, Silverman R, et al. Impact of metabolic indices on central artery stiffness: independent association of insulin resistance and glucose with aortic pulse wave velocity. Diabetologia 2010;53(6):1190-1198.
57. Poon AK, Meyer ML, Tanaka H, et al. Association of insulin resistance, from mid-life to late-life, with aortic stiffness in late-life: the Atherosclerosis Risk in Communities Study. Cardiovasc Diabetol 2020;19(1):11.
58. Safar ME, Levy BI, Struijker-Boudier H. Current perspectives on arterial stiffness and pulse pressure in hypertension and cardiovascular diseases. Circulation 2003;107(22):2864-2869.
59. Westenberg JJ. CMR for Assessment of Diastolic Function. Curr Cardiovasc Imaging Rep 2011;4(2):149-158.
60. Paulus WJ, Tschope C. A novel paradigm for heart failure with preserved ejection fraction: comorbidities drive myocardial dysfunction and remodeling through coronary microvascular endothelial inflammation. J Am Coll Cardiol 2013;62(4):263-271.
61. Fontes-Carvalho R, Pimenta J, Bettencourt P, Leite-Moreira A, Azevedo A. Association between plasma leptin and adiponectin levels and diastolic function in the general population. Expert Opin Ther Targets 2015;19(10):1283-1291.
62. Zile MR, Gottdiener JS, Hetzel SJ, et al. Prevalence and significance of alterations in cardiac structure and function in patients with heart failure and a preserved ejection fraction. Circulation 2011;124(23):2491-2501.
63. Bonora E, Targher G, Alberiche M, et al. Homeostasis model assessment closely mirrors the glucose clamp technique in the assessment of insulin sensitivity: studies in subjects with various degrees of glucose tolerance and insulin sensitivity. Diabetes Care 2000;23(1):57-63.
64. Johansson E, Lubberink M, Heurling K, et al. Whole-Body Imaging of Tissue-specific Insulin Sensitivity and Body Composition by Using an Integrated PET/MR System: A Feasibility Study. Radiology 2018;286(1):271-278.
65. Ashrafpoor G, Bollache E, Redheuil A, et al. Age-specific changes in left ventricular diastolic function: a velocity-encoded magnetic resonance imaging study. Eur Radiol 2015;25(4):1077-1086.
66. Buss SJ, Krautz B, Schnackenburg B, et al. Classification of diastolic function with phase-contrast cardiac magnetic resonance imaging: validation with echocardiography and age-related reference values. Clin Res Cardiol 2014;103(6):441-450.
67. Rathi VK, Doyle M, Yamrozik J, et al. Routine evaluation of left ventricular diastolic function

by cardiovascular magnetic resonance: a practical approach. J Cardiovasc Magn Reson 2008;10:36.
68. Nagueh SF, Smiseth OA, Appleton CP, et al. Recommendations for the Evaluation of Left Ventricular Diastolic Function by Echocardiography: An Update from the American Society of Echocardiography and the European Association of Cardiovascular Imaging. J Am Soc Echocardiogr 2016;29(4):277-314.
69. Mancusi C, de Simone G, Best LG, et al. Myocardial mechano-energetic efficiency and insulin resistance in non-diabetic members of the Strong Heart Study cohort. Cardiovasc Diabetol 2019;18(1):56.

SUPPLEMENTARY MATERIAL

Image acquisition

VAT and aSAT were assessed by acquiring three transverse images at the level of the fifth lumbar vertebra, using a turbo spin-echo protocol, with imaging parameters: repetition/echo time (TR/TE) 300/20 ms, flip angle (FA) 90°, slice thickness 10 mm, slice gap 2 mm.

For LV structure and systolic function, the LV was imaged in short-axis orientation using electrocardiographically (ECG)-gated breath-hold balanced steady-state free precession (bSSFP), with imaging parameters: TR/TE 3.4/1.7 ms, FA 35º, slice thickness 10 mm, no slice gap, field of view (FOV) 400x400 mm, matrix size 256x256.

To determine diastolic function, an ECG-gated gradient echo sequence with velocity encoding over the mitral valve was used, with imaging parameters: TR/TE 6.5/1 ms, FA 20°, slice thickness 8 mm, FOV 350x350 mm, matrix size 256x256, velocity-encoding gradient 150 cm/s, number of phases 40.

Aortic PWV was derived from retrospectively ECG-gated gradient echo sequences with velocity-encoding (200 cm/s), acquired perpendicular to the ascending and proximal descending aorta and distal descending aorta (just above the aortic bifurcation). Aortic PWV was calculated by dividing the aortic path length by the transit time of the arrival of the systolic wave front, as previously described (1).

REFERENCES

1. Widya RL, de Mutsert R, Westenberg JJM, Gast KB, den Heijer M, le Cessie S, et al. Is Hepatic Triglyceride Content Associated with Aortic Pulse Wave Velocity and Carotid Intima-Media Thickness? The Netherlands Epidemiology of Obesity Study. Radiology 2017;285:73-82.

Supplemental Table 1. Associations of HOMA-IR, VAT, aSAT and TBF with cardiovascular parameters in the total population

	Standardized difference in cardiovascular parameters (95%CI)	
	Crude	**Adjusted**
LV structure		
LV mass, g		
Log HOMA-IR	-4.0 (-6.0 to -2.0)	-4.1 (-6.4 to -1.9)
VAT (SD: 54 cm^2)	-1.9 (-3.2 to -0.5)	-3.3 (-5.1 to -1.6)
aSAT (SD: 94 cm^2)	-2.4 (-3.6 to -1.3)	-2.5 (-4.0 to -1.0)
TBF (SD: 8%)	-0.8 (-2.2 to 0.6)	0.6 (-1.7 to 2.9)
LV end-diastolic volume, mL		
Log HOMA-IR	-8.6 (-11.4 to -5.8)	-8.5 (-11.5 to -5.5)
VAT (SD: 54 cm^2)	-6.1 (-8.3 to -4.0)	-8.9 (-11.7 to -6.1)
aSAT (SD: 94 cm^2)	0.8 (-1.1 to 2.7)	-0.5 (-2.9 to 1.8)
TBF (SD: 8%)	3.5 (1.2 to 5.8)	5.4 (1.1 to 9.7)
LV concentricity, g/mL		
Log HOMA-IR	0.02 (0.01 to 0.04)	0.01 (-0.01 to 0.02)
VAT (SD: 54 cm^2)	0.03 (0.02 to 0.04)	0.02 (0.00 to 0.03)
aSAT (SD: 94 cm^2)	-0.02 (-0.03 to -0.01)	-0.01 (-0.03 to 0.00)
TBF (SD: 8%)	-0.04 (-0.05 to -0.03)	-0.02 (-0.04 to 0.00)
LV function		
LV ejection fraction, %		
Log HOMA-IR	-0.2 (-0.9 to 0.4)	0.0 (-0.8 to 0.8)
VAT (SD: 54 cm^2)	-0.3 (-0.8 to 0.1)	0.1 (-0.6 to 0.7)
aSAT (SD: 94 cm^2)	-0.5 (-0.9 to -0.1)	-0.7 (-1.2 to -0.1)
TBF (SD: 8%)	0.1 (-0.4 to 0.5)	-0.8 (-1.6 to 0.0)
E/A ratio		
Log HOMA-IR	-0.18 (-0.24 to -0.12)	-0.11 (-0.17 to -0.05)
VAT (SD: 54 cm^2)	-0.12 (-0.16 to -0.08)	-0.04 (-0.09 to 0.01)
aSAT (SD: 94 cm^2)	-0.04 (-0.08 to 0.00)	-0.05 (-0.10 to 0.00)
TBF (SD: 8%)	-0.05 (-0.09 to 0.00)	-0.09 (-0.16 to -0.02)
Aortic stiffness		
Total aorta, m/s		
Log HOMA-IR	0.2 (0.0 to 0.4)	0.0 (-0.1 to 0.2)
VAT (SD: 54 cm^2)	0.1 (0.0 to 0.2)	0.0 (-0.1 to 0.1)
aSAT (SD: 94 cm^2)	0.0 (-0.1 to 0.1)	0.0 (-0.2 to 0.1)
TBF (SD: 8%)	0.2 (0.0 to 0.3)	0.0 (-0.2 to 0.1)

Supplemental Table 1. Associations of HOMA-IR, VAT, aSAT and TBF with cardiovascular parameters in the total population

	Standardized difference in cardiovascular parameters (95%CI)	
	Crude	**Adjusted**
Aortic arch, m/s		
Log HOMA-IR	0.2 (0.0 to 0.4)	0.0 (-0.4 to 0.3)
VAT (SD: 54 cm^2)	0.2 (0.1 to 0.4)	0.0 (-0.3 to 0.2)
aSAT (SD: 94 cm^2)	0.1 (-0.1 to 0.2)	0.1 (-0.1 to 0.3)
TBF (SD: 8%)	0.1 (-0.1 to 0.3)	0.2 (-0.1 to 0.5)
Descending aorta, m/s		
Log HOMA-IR	0.2 (-0.1 to 0.4)	0.1 (-0.2 to 0.3)
VAT (SD: 54 cm^2)	0.1 (-0.1 to 0.2)	0.0 (-0.2 to 0.2)
aSAT (SD: 94 cm^2)	0.0 (-0.1 to 0.2)	-0.1 (-0.3 to 0.1)
TBF (SD: 8%)	0.2 (0.1 to 0.4)	-0.1 (-0.5 to 0.2)
Hemodynamics		
Stroke volume, mL		
Log HOMA-IR	-5.4 (-7.4 to -3.5)	-5.1 (-7.2 to -3.0)
VAT (SD: 54 cm^2)	-4.1 (-5.6 to -2.6)	-5.6 (-7.5 to -3.7)
aSAT (SD: 94 cm^2)	-0.3 (-1.6 to 1.0)	-1.4 (-2.9 to 0.2)
TBF (SD: 8%)	1.6 (0.0 to 3.2)	2.2 (-0.5 to 4.9)
Cardiac output, mL		
Log HOMA-IR	-24 (-172 to 124)	-30 (-210 to 150)
VAT (SD: 54 cm^2)	-115 (-227 to -2)	-223 (-359 to -88)
aSAT (SD: 94 cm^2)	34 (-57 to 125)	-13 (-121 to 94)
TBF (SD: 8%)	155 (37 to 273)	242 (66 to 419)

Results represent regression coefficients per 10-fold increase in HOMA-IR or per SD of measure of adiposity. In the left column, regression coefficients for LV structure and volumes (LV mass, LV end-diastolic volume, LV stroke volume and cardiac output) are corrected for lean body mass. In the right column, regression coefficients are corrected for age, sex, ethnicity, education, smoking, physical activity, use of hormone therapy, menopausal state, hypertension, lean body mass and adiposity (HOMA-IR is adjusted for VAT and TBF, VAT is adjusted for TBF, and aSAT and TBF are adjusted for VAT). Abbreviations: aSAT: abdominal subcutaneous adipose tissue, E/A ratio: ratio of mitral early and late peak filling rate, log HOMA-IR: log-transformation of the homeostatic model assessment of insulin resistance, LV: left ventricle, LV concentricity: LV mass-to-volume ratio, PWV: pulse wave velocity, TBF: total body fat, VAT: visceral adipose tissue. All analyses are weighted towards the BMI distribution of the general population (n=914). Due to missing values, for PWV total aorta: n=911, PWV descending aorta: n=832.

Supplemental Table 2. Associations of HOMA-IR, VAT, aSAT and TBF with LV mass and volumes indexed to height$^{2.7}$

	Standardized difference in cardiovascular parameters (95%CI)	
	Crude	**Adjusted**
LV mass/height$^{2.7}$, g/m$^{2.7}$		
Log HOMA-IR	0.1 (-0.5 to 0.7)	-0.8 (-1.4 to -0.2)
VAT (SD: 54 cm^2)	1.0 (0.6 to 1.3)	-0.2 (-0.7 to 0.3)
aSAT (SD: 94 cm^2)	-0.1 (-0.4 to 0.2)	0.3 (0.0 to 0.7)
TBF (SD: 8%)	-0.7 (-1.0 to -0.4)	0.6 (-0.1 to 1.3)
LV end-diastolic volume/height$^{2.7}$, L/m$^{2.7}$		
Log HOMA-IR	-0.8 (-1.6 to -0.1)	-1.6 (-2.5 to -0.8)
VAT (SD: 54 cm^2)	0.0 (-0.5 to 0.5)	-1.0 (-1.7 to -0.3)
aSAT (SD: 94 cm^2)	1.0 (0.5 to 1.5)	1.4 (0.8 to 1.9)
TBF (SD: 8%)	0.7 (0.2 to 1.2)	2.1 (0.9 to 3.3)
Stroke volume/height$^{2.7}$, mL/m$^{2.7}$		
Log HOMA-IR	-0.6 (-1.1 to -0.1)	-1.0 (-1.6 to -0.4)
VAT (SD: 54 cm^2)	-0.1 (-0.4 to 0.2)	-0.6 (-1.1 to -0.2)
aSAT (SD: 94 cm^2)	0.5 (0.1 to 0.8)	0.6 (0.2 to 1.0)
TBF (SD: 8%)	0.4 (0.1 to 0.8)	1.0 (0.3 to 1.8)
Cardiac output/height$^{2.7}$, mL/m$^{2.7}$		
Log HOMA-IR	28 (-7 to 63)	-1 (-41 to 40)
VAT (SD: 54 cm^2)	14 (-9 to 36)	-18 (-50 to 13)
aSAT (SD: 94 cm^2)	44 (22 to 65)	45 (20 to 70)
TBF (SD: 8%)	42 (19 to 65)	79 (32 to 125)

Results represent regression coefficients per 10-fold increase in HOMA-IR or per SD of measure of adiposity. Adjusted regression coefficients are corrected for age, sex, ethnicity, education, smoking, physical activity, use of hormone therapy, menopausal state, hypertension, lean body mass and adiposity (HOMA-IR is adjusted for VAT and TBF, VAT is adjusted for TBF, and aSAT and TBF are adjusted for VAT). For abbreviations, see Supplemental Table 1.